Optics and Spectroscopy, 2025, Vol. 133, No. 5

02

The influence of the structure of tetradentate phosphonates on the stability constants of their complexes with f-elements (La, Nd, Eu, Lu, and Th)

© Ts.B. Sumyanova, A.A. Kirsanova, N.E. Borisova

Moscow State University, Moscow, Russia

e-mail: ts.sumyanova90@gmail.com

Received December 10, 2024
Revised January 20, 2025
Accepted April 07, 2025

The influence of the central metal ion on the stability constants of complexes of thorium, lanthanum, neodymium, europium, and lutetium with phosphonate ligands based on 2, 2′-bipyridine and 1, 10′-phenanthroline has been studied. Solutions in acetonitrile were investigated using spectrophotometric titration at a constant temperature of $25 \pm 0.1^\circ$C. Absorption spectra were obtained for the studied phosphonate ligands and their complexes. The metal-to-ligand ratios in the formed complexes were determined using spectrophotometric titration curves and the method of isomolar series. Factor analysis was used to determine the number of independent absorbing components in the chemical system. The stability constants of lanthanide and thorium complexes with phosphonate ligands were calculated using the HypSpec2014 program. Dependence curves of the complex stability constants on the ionic radii of the metals were plotted.

Keywords: complex stability constant, f-elements, lanthanides, thorium.

DOI: 10.61011/EOS.2025.05.61638.21-25

1. Introduction

Thorium and lanthanide compounds are widely used as refractory materials [1], optical and electrochemical sensors [2,3]. Much attention is paid to the development of fluorescent probes for the detection and quantification of their content in the field [2,4,5]. Detection of thorium ions (Th^{4+}) among lanthanide ions becomes a difficult task due to the proximity of their ionic radii. A highly sensitive fluorescent probe was developed in the study in Ref. [6] for detection of thorium (IV) ions in real water samples and showed excellent selectivity and sensitivity to thorium ions (Th^{4+}) compared to other competing metal ions. The successful application of the developed sensor probe for the recognition of thorium ions in E.coli cells was also reported in Ref. [6].

The demand for energy for industry and high-performance computing is growing with the growth of the world's population and the exponential growth of industry. Currently, fossil fuels such as natural gas, oil and coal do not have analogues that could meet the current demand for energy at an acceptable cost. The nuclear energy is one of the solution for the global energy crisis. If functioning nuclear reactors are completely replaced by fast neutron reactors, then nuclear power can be considered as a sustainable source of clean energy. High energy intensity and low greenhouse gas emissions are the main advantages of nuclear energy. According to studies in Ref. [7–9], over the past twenty years, approximately 11 to 20% of the world's energy needs have been met through nuclear energy. According to calculations by the International Atomic Energy Agency, a nuclear reactor with a capacity of 1,000 MW will annually produce about 30 tons of high level solid waste (HLSW). At the same time, a coal-fired power plant of similar capacity produces 300,000 tons of ash annually [10]. The amount of HLSW produced by nuclear power plants is significantly less than the amount of waste from other methods of electricity production. The disadvantages include the possibility of radioactive contamination and the problem of storing radioactive waste. Thus, proper management of HLSW and spent nuclear fuel (SNF) and their safe decommissioning are among the main problems of electricity generation at nuclear power plants. The SNF waste account for the largest proportion of high-level nuclear waste in different countries that apply an open fuel cycle strategy. Spent nuclear fuel can be considered either as waste that will eventually be packaged and disposed of, or as recyclable raw materials for the extraction of uranium and plutonium, followed by the preparation of highly radioactive waste containing mainly fission and activation products (minor actinides). In some countries, liquid waste immobilization is chosen instead of SNF processing, where the waste is converted to solid form through vitrification and deep geological burial, which will lead to an increase in the volume of SNF as the use of nuclear energy increases. Nuclear waste recycling is the most effective method of solving this problem, as it reduces waste disposal time by a factor of 100 and reduces storage capacity by a factor of 4–6 [10].

More and more attention is paid to thorium fuel due to the continued consumption of uranium resources, since ^{232}Th can be converted into ^{233}U by absorbing slow neutrons [7,11]. Monazite and xenotime are ores of rare earth elements and thorium. Thorium fuel reactors should include appropriate reprocessing technology in their design. The process of reprocessing spent fuel from thorium-fueled reactors has been developed based on PUREX technology (plutonium-uranium recovery by extraction, water extraction or extraction-sorption technology based on tributyl phosphate (TBP)). The THOREX (thorium-uranium extraction) spent thorium fuel reprocessing process includes the joint extraction of uranium-233 and thorium. The process is based on solvent extraction of thorium and uranium using TBP and is considered the most efficient way to extract uranium and thorium.

The extraction and separation of lanthanides and thorium is necessary for the disposal of highly radioactive waste. The fractionation with the release of long-lived and radiotoxic nuclides, followed by separation into separate fractions in accordance with half-lives and chemical behavior is one of the strategies for handling them. Then, particularly strong matrices are created for each fraction for safe burial. The fractionation technology has a problem in the extraction separation of actinides and lanthanides due to the proximity of chemical properties, including ionic radii. For example, the ionic radii of cations are very close; among lanthanides, there are isostructural analogues of americium and curium cations present in HLSW: $r(Am^{3+}) \sim r(Nd^{3+})$. This complicates the separation of minor actinides and lanthanides by existing methods. Lanthanides and actinides are elements that preferentially bind to heavy oxygen donor atoms in the complexation reaction. Complexation is a useful tool for separating metal ions if it is used for systems consisting of two immiscible liquid phases. In such cases, the selectivity of complexation is a valuable characteristic, therefore, knowledge of the stability constants of f-element complexes is necessary to study the extraction separation of actinides and lanthanides. A good correlation was observed in Ref. [12] between the distribution coefficients and stability constants of methyl-substituted BPDA complexes (N6, $N6'$-diethyl-N6, $N6'$-bis(R-phenyl)-2, 2′-bipyridine]-6, 6′-dicarboxamides) with lanthanides in „dry“ acetonitrile (with water content of 40 ± 5 ppm).

The authors suggested that the separation of light lanthanides is mainly determined by the stability constant of the corresponding complexes and, to a lesser extent, by the hydration of metal ions. In contrast, the separation of heavy lanthanides is better explained by taking into account the effects of hydration. In this regard, the following metals were selected for the study: thorium, lanthanum, lutetium, neodymium and europium. Thorium, in turn, belongs to a number of actinides, since thorium-232 is the most common natural isotope of thorium. Europium has similar properties to americium. Six electrons are located in $4f$- and $5f$-orbitals, respectively, in the europium ion and the Americium ion. The neodymium ion is often compared to americium and curium ions because their ionic radii are very close. Lanthanum and lutetium are located at the beginning and end, respectively, in the lanthanide series.

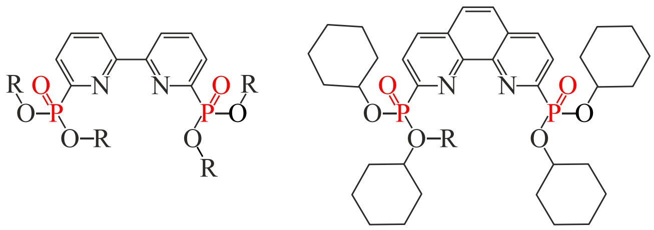

Figure 1. Structure on the left: tetraR[2, 2′-bipyridine]-6, 6′-diyl bis(phosphonate); radical R = isopropyl (iPr), cyclohexyl (cHex). The structure on the right is tetracyclohexyl-1,10-phenanthroline-2,9-diyl bis(phosphonate). Designations: 1,10-phenanthroline = phen, [2, 2′-bipyridine] = bipy. Next, the structure on the left: bipy-PO-(OiPr)4, bipy-PO-(OcHex)$_4$; the structure on the right: phen-PO-(OcHex)$_4$.

2. Objects and methods of research

The structures of the studied compounds are shown in Fig. 1 (the synthesis is described in Ref. [13]). Acetonitrile (99.95%, Biosolve) was used as a solvent for spectrophotometric studies. Acetonitrile was previously dried over molecular sieves (zeolite KA, 3,AA, HKC Corp.) to maintain a constant water content in the solvent. The water content in the solvent was determined using the Karl Fischer method using a Karl Fischer coulometric titrator (DL-32, MettlerToledo). The water content in acetonitrile was 40 ± 5 ppm. Metal nitrate crystallohydrates $M(NO_3)_x \cdot nH_2O$ (M = La, Nd, Eu, Lu, Th, where $x = 3$, 4, $n = 4-6$, purity > 99%, IREA). Absorption spectra were recorded in the wavelength range 200−500 nm (with 1 nm interval) using a Hitachi U−1900 spectrophotometer in a 10 mm quartz spectrophotometric cuvette (Hellma). A constant temperature of 25 ± 0.1°C was maintained in the cuvette using circulation bath with a temperature controller (Model 1162A, VWR).

The analytical absorption wavelength of the complex (λ_{an}) for determining its composition was measured using the Firordt method as $A_x - A_L = f(\lambda)$, where A_x is the optical density of a mixture of ligand and metal solutions (see above), A_L is the optical density of the free ligand solution. The wavelength value corresponding to the maximum on the constructed curve $f(\lambda)$ was taken as λ_{an}. Solutions of ligands (bipy-PO-(OiPr)$_4$, bipy-PO-(OcHex)$_4$ and phen-PO-(OcHex)$_4$), salts of metal nitrates (La, Nd, Eu, Lu, Th) were prepared for determining the time of chemical equilibrium. The optical density of an equivalent mixture of solutions of ligands and salts of metal nitrates was recorded for 15 min (900 s) at the absorption wavelength of the complex (for bipy-PO-(OiPr)$_4$, bipy-PO-(OcHex)$_4$ − 300 nm, for phen-PO-(OcHex)$_4$ − 286 nm), using acetonitrile as a reference solution. The time of establishment of equilibrium in the system is defined as the moment after which no further change in optical density is observed.

Solutions of metal ligands and nitrates in acetonitrile were prepared by weighing precise weights of ligands and metal nitrate crystallohydrates. A solution of the ligand ($2 \cdot 10^{-5}$ M) was placed in the cuvette for determining the equilibrium constant of the complexation reaction. Suspensions of metal nitrate salts are prepared in a ligand solution. After that, aliquots of the metal nitrate salt solution ($2 \cdot 10^{-3}$ M) were added to the cuvette. Absorption spectra were recorded after each addition of a metal nitrate solution until an excess of 3 equivalent metal salt was reached.

Based on the equations of material balance, Booger–Lambert–Beer law and the law of additivity of optical densities, equations are derived for calculating the equilibrium concentrations of the complex, ligand, and metal (the charge of the metal ion is omitted for convenience) [14–19]. The equilibrium constant K is calculated by the equation: $K = [\mathrm{ML}][\mathrm{L}]^{-1}[\mathrm{M}]^{-1}$. The obtained spectrophotometric data were processed using the HypSpec 2014 program [14]. This program takes into account the present reagents and equilibrium constants nk. The objective function is given in matrix notation as $U = r^T W r$, where r is the remainder vector, $r = (y^{\mathrm{obt}} - y^{\mathrm{calc}})$, y are optical density matrices, W is the weight matrix. The target function was minimized by using the Gauss–Newton–Marquardt method generalized by the system of equations

$$(J^{\mathrm{T}}WJ + \lambda D)\Delta p = J^{\mathrm{T}}Wr,$$

where J is the Jacobian, Δp is the vector of shifts to be applied to the parameters, D is assumed to be equal to the diagonal elements $J^{\mathrm{T}}Wr$, λ is the Marquardt parameter. The Jacobian elements are obtained from the equations of Bouguer–Lambert–Beer law:

$$A_\lambda = l \sum_{j=l,na} \varepsilon_{i,j} c_j,$$

$$\frac{\partial A_\lambda}{\partial x} = l \sum_j \varepsilon_{\lambda,j} \frac{\partial c_j}{\partial x},$$

Jacobian

$$\begin{array}{ccccccccc}
0 & \dots & 0 & 0 & \dots & 0 & 0 & \dots & 0 \\
\frac{\partial A_1}{\partial \varepsilon_{1,1}} & \dots & \frac{\partial A_1}{\partial \varepsilon_{1,na}} & 0 & \dots & 0 & 0 & \dots & 0 \\
0 & \dots & 0 & \frac{\partial A_2}{\partial \varepsilon_{2,1}} & \dots & \frac{\partial A_2}{\partial \varepsilon_{2na}} & \frac{\partial A_2}{\partial \varepsilon_{2,na}} & \dots & 0 \\
\vdots & \dots & \vdots & \vdots & \dots & \vdots & \vdots & \dots & \vdots \\
0 & \dots & 0 & 0 & \dots & 0 & 0 & \dots & \frac{\partial A_{nl}}{\partial \varepsilon_{ml,1}}.
\end{array}$$

In addition, the system is subject to the condition of fulfilling the equations of the material balance:

$$T_{\mathrm{M}} = [\mathrm{M}] + \sum_{k=1,nk} p_k \beta_k [\mathrm{M}]^{p_k} [L]^{q_k} [\mathrm{ML}]^{r_k} = [\mathrm{M}] + \sum p_k c_k.$$

This equation is for the salt of metal nitrate ($\mathrm{M(NO_3)}_x \cdot n\mathrm{H_2O}$), similar equations are made for L and ML. Moreover, the total concentration of TM is

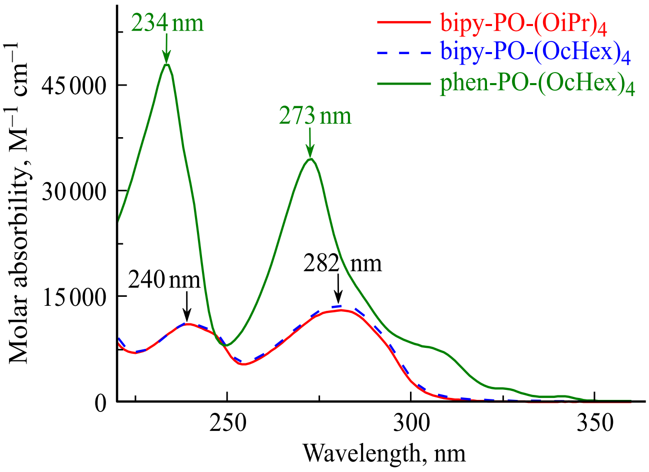

Figure 2. Phosphonate absorption spectra: bipy-PO-(OiPr)$_4$ (red curve), bipy-PO-(OcHex)$_4$ (blue dashed curve), phen-PO-(OcHex)$_4$ (green curve).

obtained based on the initial amount of the substance n_{M}, the concentration in the burette a_{M}, the initial volume v_0 and the added volume of the aliquot v. Thus, the three equations of the material balance have the form

$$\frac{n_{\mathrm{M}} + v a_{\mathrm{M}}}{v_0 + v} = [\mathrm{M}] + \sum_{k=1,nk} p_k c_k,$$

$$\frac{n_{\mathrm{L}} + v a_{\mathrm{L}}}{v_0 + v} = [\mathrm{L}] + \sum_{k=1,nk} q_k c_k,$$

$$\frac{n_{\mathrm{ML}} + v a_{\mathrm{ML}}}{v_0 + v} = [\mathrm{ML}] + \sum_{k=1,nk} r_k c_k.$$

The number of independent absorbing components in a solution can be determined in HypSpec 2014 using the method of factor analysis of the matrix of experimental values of optical densities [15]. Each absorbing component of the solution has a „single“ spectrum, which is a spectrum for a single concentration and a single optical path length. In this case, the number of nonzero eigenvalues will be equal to the number of independent absorbing components of the chemical system.

The stoichiometry of the complex was confirmed using the isomolar series method (the Ostromyslensky–Zhoba method) [18,19], where the ratio of isomolar concentrations of reactants (only the ratio $m:n$) corresponds to the maximum yield of the complex compound $\mathrm{M}_m\mathrm{L}_n$. The analysis was performed by preparing solutions of both components (reagent and metal) of the same molar concentration and mixing them in ratios (most often from 1 : 9 to 9 : 1), keeping the total volume of the solution unchanged ($V_{\mathrm{M}} + V_{\mathrm{L}} = V = \mathrm{const}$). At the same time, the total number of moles of both components in the total volume of the mixture always remains constant ($C_{\mathrm{M}} + C_{\mathrm{L}} = C = \mathrm{const}$).

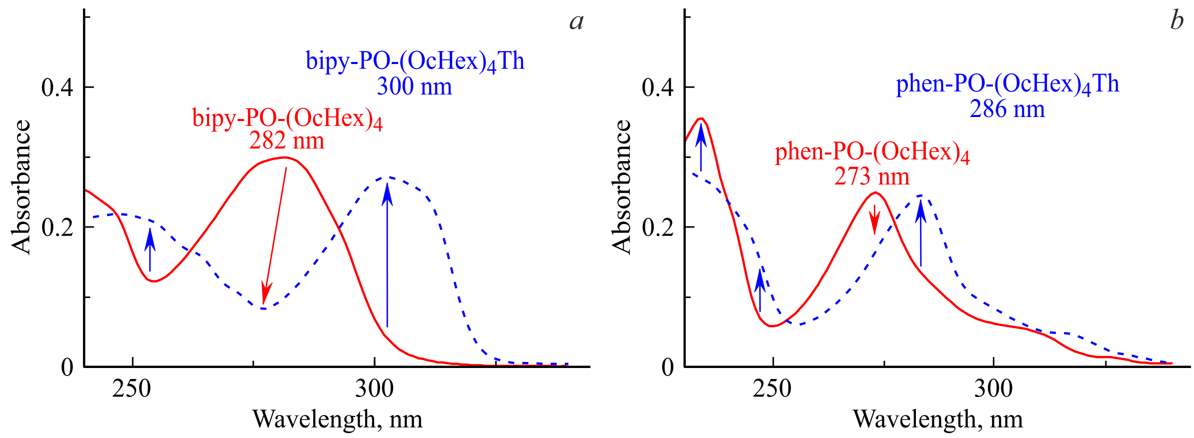

Figure 3. Changes in the absorption spectra of solutions during complex formation: ligand solution (solid curve), added excess thorium nitrate crystallohydrate (dashed curve); (*a*) formation of a thorium complex with the bipy-PO-$(OcHex)_4$ ligand, (*b*) formation of a thorium complex with the phen-PO-$(OcHex)_4$ ligand.

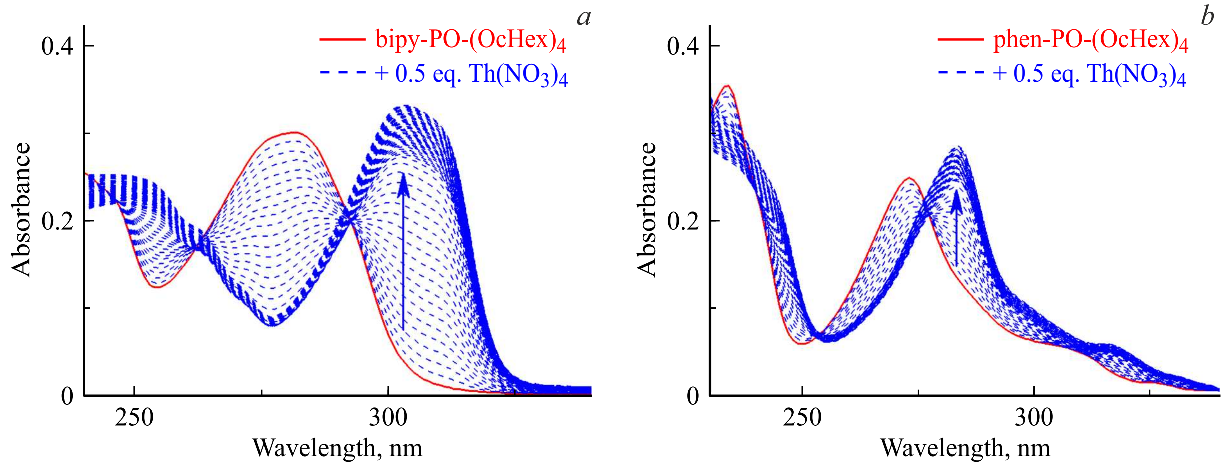

Figure 4. Spectrophotometric data: 0.5 thorium equivalents were added to the phosphonate, titration was carried out to 3 equivalents; (*a*) bipy-PO-$(OcHex)_4$, (*b*) phen-PO-$(OcHex)_4$.

When low-stability complex compounds are formed, there will be no sharp break in the curves. The maximum is determined by extrapolating the sections of the curve corresponding to an excess of one of the components in the solution, which contributes to a shift in equilibrium towards the formation of a complex.

3. Experimental results

3.1. Absorption spectra

The absorption spectra of phosphonates are shown in Fig. 2, where, two peaks were observed at wavelengths of 240 and 282 nm regardless of the substituent in the structure of 2, 2′-bipyridine ligand (bipy-PO). At wavelengths of 234 and 273 nm for tetracyclohexyl-1,10-phenanthroline phosphonate (phen-PO-$(OcHex)_4$). The addition of metal nitrate crystallohydrate to the ligands resulted in a bathochromic shift of 18 nm for 2, 2′-bipyridine phosphonates (Fig. 3, *a*) and 13 nm for 1, 10′-phenanthroline-phosphonate (Fig. 3, *b*). The stability constants of complexes of metal nitrate salts with phosphonates were determined by spectrophotometric titration. Fig. 4 shows examples of spectrophotometric titrations between thorium nitrate salts with phosphonates (respectively, bipy-PO-$(OcHex)_4$ and phen-PO-$(OcHex)_4$). A kinetic experiment was performed for bipyridine phosphonates at a wavelength of 300 nm and for phenanthroline phosphonate at 286 nm. It was found that the equilibrium in the complexation reaction is established quickly, and the absorption is stabilized during 5−10 s regardless of the studied metal nitrate salt.

3.2. Composition of the complex in solution

The composition of the equilibrium solution was determined using the titrimetric method, the method of factor analysis and the method of isomolar series. Using the titrimetric method (Fig. 5, *a* and 6, *a*), it was found that

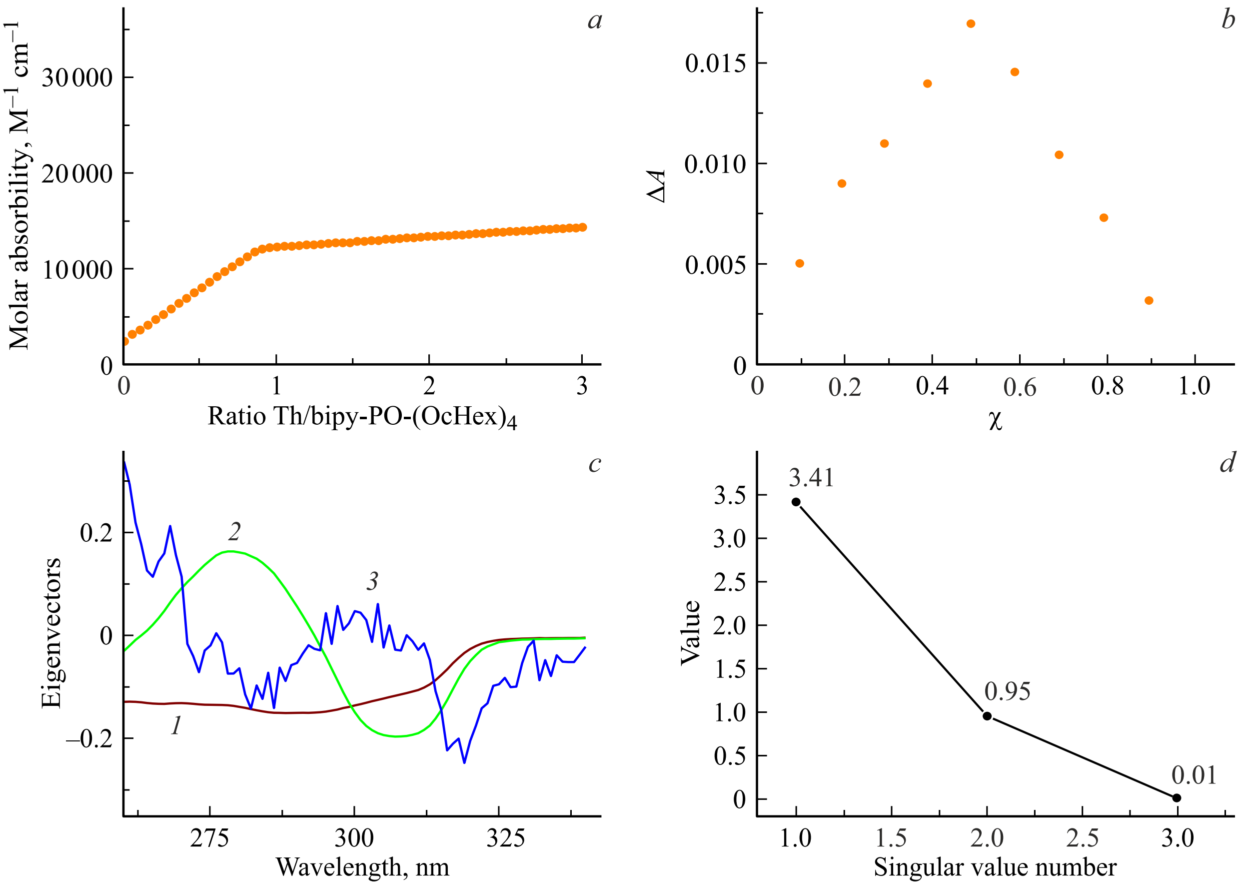

Figure 5. Determination of the composition of the bipy-PO-(OcHex)$_4$ ligand complex with thorium nitrate using the following methods: (*a*) titration curve; (*b*) isomolar series; factor analysis — (*c*) eigenvectors (where *1–3* — unit spectra), (*d*) eigenvalues (where values are — eigenvalues in factor analysis).

there is a sharp bend in the titration curves at the first equivalent of the added metal salt. This indicates that the composition of the complexes corresponds to the metal-ligand ratio 1 : 1. This is also additionally confirmed by the isomolar series method, where Figures 5, *b* and 6, *b* show a sharp break at a ratio of 0.5, which indicates the formation of only one high-strength metal-ligand complex 1 : 1. The method of factor analysis of optical density matrices for each of the studied systems was used to show that three independent absorbing components are present in the solution: a free ligand, a free metal, and a complex in Fig. 5, *c, d* and 6, *c, d*.

3.3. Stability of complexes

The stability constants of complexes between metal nitrate crystallohydrates and phosphonates were determined by spectrophotometric titration and processed using the HypSpec 2014 program. The calculated stability constants of the complexes are presented in the table and in Fig. 7 in comparison with the previously published constants of complexes with neodymium and europium nitrates [13]. The ionic radii of lanthanides and thorium were taken from Ref. [20,21] to illustrate the dependence of the stability constants of complexes on the ionic radius of the metal. The comparison of the stability constants of thorium complexes with isopropyl-substituted ligand (bipy-PO-(OiPr)$_4$) ($\lg\beta_{\mathrm{ThL}} = 7.62 \pm 0.05$) and a cyclohexyl-substituted ligand (bipy-PO-(OcHex)$_4$) ($\lg\beta_{\mathrm{ThL}} = 7.08 \pm 0.03$) showed that the stability values of the complexes are almost close with a difference of 0.46 orders of magnitude. This was observed in Ref. [13] for the stability constants of neodymium complexes with cyclohexyl-substituted ligand (bipy-PO-(OcHex)$_4$) ($\lg\beta_{\mathrm{NdL}} = 7.52 \pm 0.06$) and isopropyl-substituted ligand (bipy-PO-(OiPr)$_4$) ($\lg\beta_{\mathrm{NdL}} = 6.79 \pm 0.03$) with a difference in 0.64 orders of magnitude. It also follows from the table that the stability constants of the complexes bipy-PO-(OiPr)$_4$ and bipy-PO-(OcHex)$_4$) with lanthanum (respectively $\lg\beta_{\mathrm{LaL}} = 7.51 \pm 0.07$ and $\lg\beta_{\mathrm{LaL}} = 7.38 \pm 0.09$) and lutetium (accordingly, $\lg\beta_{\mathrm{LuL}} = 7.36 \pm 0.05$ and $\lg\beta_{\mathrm{LuL}} = 7.47 \pm 0.14$) match within the margin of error. Fig. 7 showed that, regardless of the size of the substituent in the bipyridine phosphonate structure, the stability constants of lanthanide complexes are almost equal. The replacement of the structural framework of the phosphonate ligand from bipyridine to phenanthroline leads to the formation of a

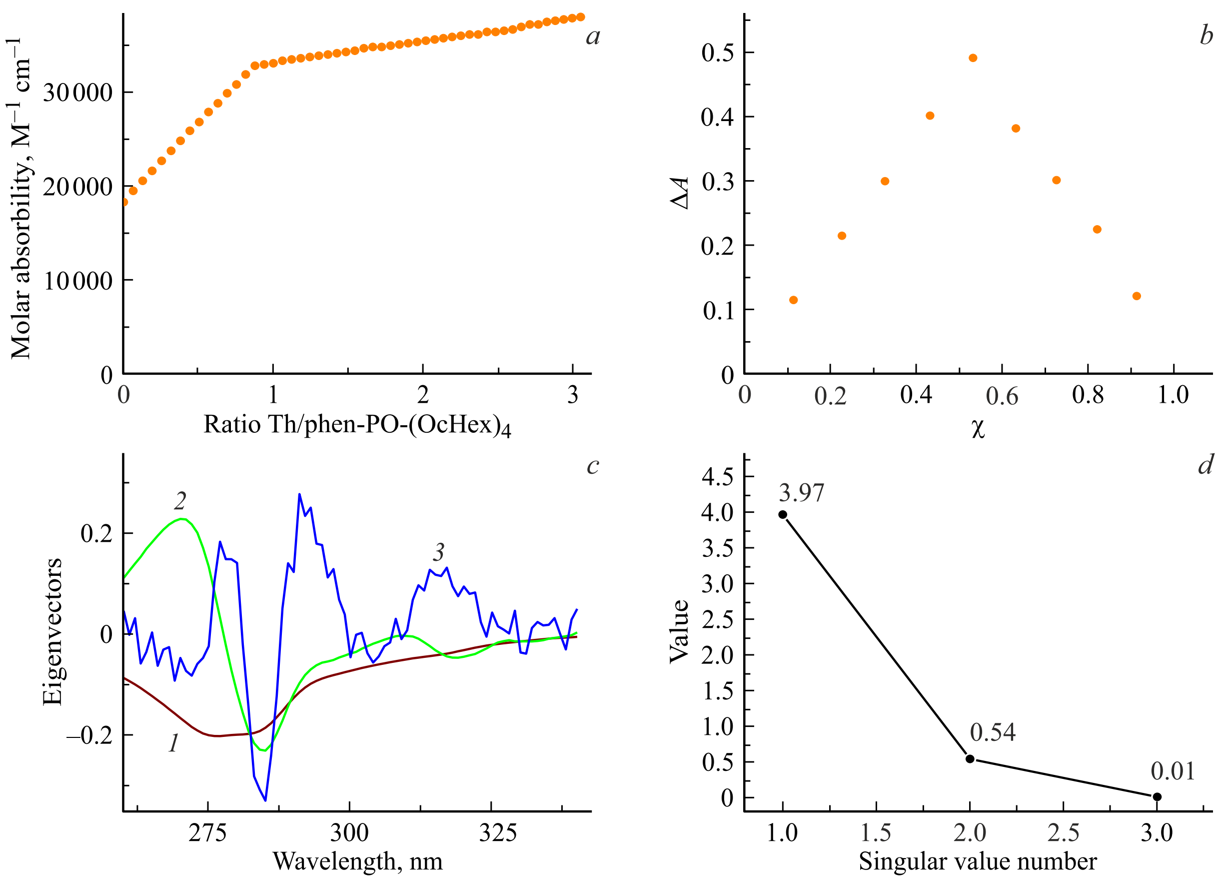

Figure 6. Determination of the composition of the phen-PO-(OcHex)$_4$ ligand complex with thorium nitrate using the following methods: (*a*) titration curve; (*b*) isomolar series; factor analysis — (*c*) eigenvectors (where *1-3* is the unit spectra), (*d*) eigenvalues (where values are the eigenvalues in factor analysis).

Stability constants of complexes with metal nitrates ($\lg\beta_{\mathrm{ML}}$)

Phosphonate	La^{3+}	Nd^{3+}	Eu^{3+}	Lu^{3+}	Th^{4+}
bipy-PO-OiPr	7.51 ± 0.07	6.79 ± 0.03 [12]	7.49 ± 0.07 [12]	7.36 ± 0.05	7.62 ± 0.05
bipy-PO-OcHex	7.38 ± 0.09	7.52 ± 0.06 [12]	7.74 ± 0.07 [12]	7.47 ± 0.14	7.08 ± 0.03
phen-PO-OcHex	6.17 ± 0.13	7.23 ± 0.07 [12]	7.54 ± 0.19 [12]	6.77 ± 0.07	6.92 ± 0.08

pronounced maximum on the europium ion on the curve of dependence of the stability constant of complexes on the ionic radius of the metal.

4. Conclusion

It has been established that, regardless of the phosphonate structure, a one-to-one metal-ligand complex is formed. The presence of a bipyridine fragment in the phosphonate structure does not lead to a significant difference in the dependence of the stability of complexes on the ionic radius, regardless of the size of the substituents in the ligand structure. Regardless of the size of the bulk substituent in the bipyridine phosphonate structure, the stability values of the complexes coincide within the margin of error. On the contrary, the presence of a phenanthroline fragment in the ligand structure leads to the formation of a maximum difference in the stability constants of complexes with the europium ion in a series of f-elements with an increase in the ionic radius of the metal. It can be assumed that the rigid structure of a phosphonate ligand based on 1,10′-phenanthroline will be most suitable for the selective separation of metal ions in the development of a new reagent.

Funding

This study was supported financially by grant No. 20-73-10076-P from the Russian Science Foundation. NMR spectra of the initial ligands were measured using equipment provided as part of the federal project „Development of

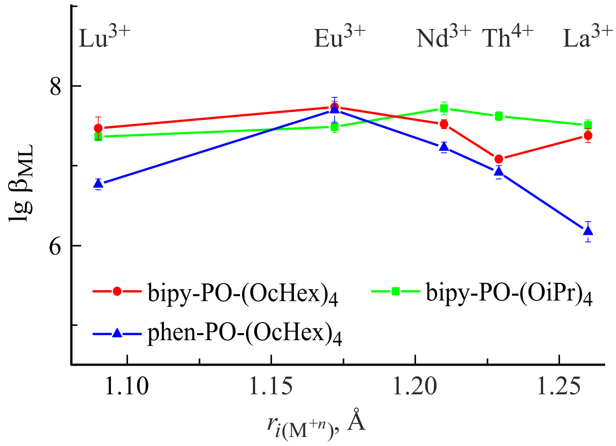

Figure 7. Dependence of the stability constants of complexes on an increase in the ionic radius of the metal.

Research and Training Infrastructure" of national project „Science and Universities" dated July 20, 2023 No 322.

Conflict of interest

The authors declare that they have no conflict of interest.

References

[1] S.V. Ushakov, Q.-J. Hong, D.A. Gilbert, A. Navrotsky, A.v.d. Walle. Materials, **16**, 1350 (2023). DOI: 10.3390/ma16041350
[2] S. Kumar, R. Bhaskar, H.K. Sharma, S.K. Ashok Kumar, S.K. Sahoo. Trends in Analytical Chemistry, **172**, 117551 (2024). DOI: 10.1016/j.trac.2024.117551
[3] H. Xiong, H. Liang, K. Dai, Q. Tian, X. Dai, H. Su, G. Royal. Spectrochim. Acta A, **293**, 122501 (2023). DOI: 10.1016/j.saa.2023.122501
[4] B. Liua, Y. Tan, Q. Hu, Y. Wang, Y. Mao, P. Tao, H. Wang. Sensors and Actuators B, **26**, 126675 (2019). DOI: 10.1016/j.snb.2019.126675
[5] Y. Fang, W. Dehaen. Coord. Chem. Rev., **427**, 213524 (2021). DOI: 10.1016/j.ccr.2020.213524
[6] Sh. Seenan, S. Manickam, S. Sawminathan, D. Jothi, S.K. Iyer. J. Photochem. Photobiol. A, **430**, 113952 (2022). DOI: 10.1016/j.jphotochem.2022.113952
[7] R.K. Jyothi, L.G.T.C. De Melo, R.M. Santos, H.-S. Yoon. Front. Energy Res., **11**, 1132611 (2023). DOI: 10.3389/fenrg.2023.1132611
[8] Qichao Zhang, Yanliang Huang, Wolfgang Sand, Xiutong Wang. Int. J. Hydr. Energy, **4**, 23 (2019). DOI: 10.1016/j.ijhydene.2019.03.154
[9] W.W. Lukens, S.A. Saslow. Chemistry of Materials, **29**, 24 (2017). DOI: 10.1021/acs.chemmater.7b03567
[10] J. Wallenius. Annals of Nuclear Energy, **125**, 74 (2019). DOI: 10.1016/j.anucene.2018.10.034
[11] Turan Ünak. Progress in Nuclear Energy, **37**, 1−4 (2000). DOI: 10.1016/S0149-1970(00)00038-X
[12] N.E. Borisova, Ts.B. Sumyanova, A.V. Kharcheva, P.I. Matveev, A.V. Ivanov, E.A. Razumova, S.V. Patsaeva. Dalton Trans., **47**, 16755−16765 (2018). DOI: 10.1039/C8DT03734E
[13] P.I. Matveev, P.-W. Huang, A.A. Kirsanova, I.V. Ananyev, Ts.B. Sumyanova, A.V. Kharcheva, E.Yu. Khvorostinin, V.G. Petrov, W.-Q. Shi, S.N. Kalmykov, N.E. Borisova. Inorg. Chem., **60**, 19 (2021). DOI: 10.1021/acs.inorgchem.1c01432
[14] P. Gans, A. Sabatini, A. Vacca. Talanta, **43**, 1739 (1996). DOI: 10.1016/0039-9140(96)01958-3
[15] R. Tauler, A. Smilde, B. Kowalski. J. Chemometr., **9**, 31 (1995). DOI: 10.1002/cem.1180090105
[16] F. Rossotti, Kh. Rossotti. *Opredeleniye konstant ustoychivosti i drugikh konstant ravnovesiya v rastvorakh* (Mir, M., 1965) (in Russian).
[17] K.A. Connors. *Binding Constants: The Measurement of Molecular Complex Stability* (Wiley, N.Y., 1987).
[18] M.I. Bulatov, I.P. Kalinkin. *Prakticheskoye rukovodstvo po fotokolorimetricheskim i spektrofotometricheskim metodam analiza* (Khimiya, L., 1986) (in Russian).
[19] G.L. Shlefer.*Kompleksoobrazovaniye v rastvorakh. Metody opredeleniya sostava i konstant ustoychivosti v rastvorakh* (Khimiya, L., 1964) (in Russian).
[20] R.D. Shannon. Acta Crystallogr. A, **32** (1976). DOI: 10.1107/S0567739476001551
[21] N. Torapava, I. Persson, L. Eriksson, D. Lundberg. Inorg. Chem., **48**, 24 (2009). DOI: 10.1021/ic901763s

Translated by A.Akhtyamov